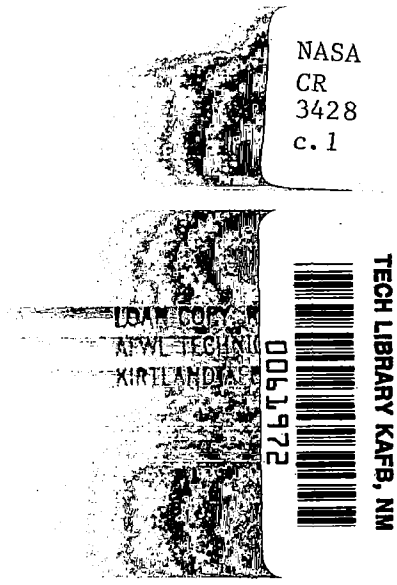

NASA Contractor Report 3428

Photoexcitation of Lasers and Chemical Reactions for NASA Missions - A Theoretical Study

A. Javan and M. Guerra

CONTRACT NAS1-14688
MAY 1981

NASA

NASA Contractor Report 3428

Photoexcitation of Lasers and Chemical Reactions for NASA Missions - A Theoretical Study

A. Javan and M. Guerra
Laser Development Corporation
Lexington, Massachusetts

Prepared for
Langley Research Center
under Contract NAS1-14688

National Aeronautics
and Space Administration

Scientific and Technical
Information Branch

1981

Table of Contents

Page

Part I - Possibility of Optically Pumped CW IR Lasers at Multi-atmospheric Gas Pressures. 1

Introduction 1

Summary of the Content 4

Subsection 1a - Hollow Waveguide for Optical Pumping 7

Subsection 1b - Waveguide Losses 9

Section 2 - Gaseous Systems Suitable for CW Optical Pumping in a Waveguide 12

Subsection 2a - CO_2 Laser as the Optical Pumping Source 13

Subsection 2b - Optical Pumping with a CW CO Laser; A Proposed Ternary Gaseous Medium 15

Estimate of gain 17

References 27

Part II - Estimates of VV and VT Rate Constants in Pure CO and NO Gases and CO-NO Gas Mixtures 28

References 38

Table I - VT Rate Constants for NO-CO 40

Table II - VT Rate Constants for CO-CO 42

Table III - VT Rate Constants for NO-NO 43

Fig. 1 - Graphs Giving VV Rates for NO-CO 44

Fig. 2 - Graphs Giving VV Rates for CO-CO 45

Fig. 3 - Graphs Giving VV Rates for NO-NO 46

Part I - Possibility of Optically Pumped CW IR Lasers at Multi-Atmospheric Gas Pressures.

Introduction

In the past several years, there have been a number of ways in which an intense infrared laser has been applied to optically pump a gaseous medium and produce gain and, hence, laser oscillation in new wavelength regions. These fall broadly into two categories: the first consists of pulsed systems in which intense laser radiation pulses are used in the optical pumping of gaseous media at pressures ranging from several mtorrs to many atmospheres. The second consists of optically pumped gaseous laser systems with the capability of operating continuously; these have all been achieved at low gas pressures where the narrow line widths give higher gains at reduced number of molecules in the laser levels.

Lasers operating at elevated gas pressures are of particular interest because of the pressure broadening of the amplifying transitions, making possible frequency tuning over broad regions.

In several cases where laser oscillation with pulsed optical pumping have been achieved at elevated gas pressures, the experiments have been performed at a low repetition rate with resultant low average output powers. A high repetition rate or CW optically pumped high pressure gas laser, however, would require taking into consideration a variety of practical as well as basic problems not encountered in transient low reptition rate systems.

The purpose of this report is to analyze the possibility of obtaining CW or high repetition rate optically pumped gaseous systems capable of operating in the pressure ranges exceeding hundreds of torrs and extending into the multi-atmospheric regions. At a pressure of several atmospheres, the full gain-bandwidth of an individual molecular rotation-vibration transition is in the ten to

twenty GHz range. Considering that in a high gain system laser oscillation can be obtained over a large number of rotation-vibration transitions, a laser operating at several atmospheres gas pressure will have frequency tuning capability over a broad region. This frequency tuning range can be further extended by isotopic substitution of the lasing molecules which due to the isotope effect will oscillate at shifted frequencies. It is also well known that in some cases, the isotopic substitution will allow new transitions to appear (due to a removal of molecular symmetry) giving rise to additional laser transitions not occurring in the lasing molecules at its natural isotopic abundance.

Optical pumping with an incident laser radiation at a moderate field intensity is a nondestructive process and does not cause molecular dissociation. This feature is particularly advantageous in operating a sealed-off laser utilizing gaseous molecules with rare isotopic constituents. This is to be contrasted with a gaseous discharge system in which molecular dissociation poses a major problem in sealed-off operation.

The objective of the analysis presented below is to point out that, with further developments, it is possible to construct a new family of frequency tunable gas laser devices covering a broad region of the infrared. These lasers can have major impact in a variety of applications, including their utilization as local oscillators for superheterodyne remote sensing of trace gases in the atmosphere.

The discussion presented below will be specifically addressed to the problem of obtaining CW laser oscillation in a high pressure gaseous medium with a CW incident optical pumping laser radiation. This would cover the less stringent high repetition rate mode of operation which can readily be achieved in the same system by operating the optical pumping laser in a repetitive Q-switched mode with peak pulse intensities considerably higher than the CW output.

To achieve sizable excitation of a high lying molecular level with optical pumping in a high pressure gas, two considerations are of basic importance: the first relates to a need to maintain the pump radiation flux at a high intensity over a sufficiently long propagation distance to produce the necessary gain-length for laser oscillation in the high pressure medium. It is important that this be achieved without heating the gas excessively. This rules out CW operation in cases where the optical pumping radiation is heavily absorbed over a short propagation length. The second relates to the choice of the high pressure gaseous systems which would allow the necessary high population densities in the laser levels to be maintained at elevated gas pressures.

With a focussed laser radiation, high radiation flux can be obtained in the focal region. With long focal length optics, this high intensity can be generated over a fairly long propagation length. In this way, a laser having a moderate output power can be used to obtain high field intensities in a pencil beam of limited cross section. Over and above this, we draw attention to the fact that in an appropriate small cross section hollow waveguide, high pump radiation flux can be maintained over propagation distances considerably longer than those obtainably in the focal region of an appropriately focussed laser radiation. Although in favorable cases the use of a waveguide may not be necessary, in principle, however, the threshold pump power may be lowered with optical pumping in a waveguide. The problem of hollow waveguides has received considerable attention in a variety of applications. A summary discussion reviewing the aspects relevant to the optical pumping problems under consideration here is presented below.

In connection with the choice of the gaseous medium for the optical pumping, the second consideration noted

above, we analyze here several systems, one of which takes advantage of the process of energy storage - energy transfer in molecular vibrations with long V-T decay times and fast V-V transfer rates. In the past, several optically pumped energy storage systems have been made to oscillate. All these previous cases, however, have required very intense pump radiation obtainable only in short duration pulses. Here we discuss a new and broadly applicable energy transfer-energy storage approach which operates on a basis fundamentally different from those known previously. In this new approach a ternary gas mixture is used in which the CW pump radiation is absorbed by one molecular species and then transferred and stored in another molecular constituent of the mixture. The stored energy is subsequently utilized to excite the laser levels of a third molecular species. The advantages of separating the pump energy absorbing molecules from the energy storing molecules are clarified below.

SUMMARY OF THE CONTENT

Section 1 gives a brief account of the previously known optically pumped gas laser systems. The discussion then shows the advantages of using a hollow waveguide for CW optical pumping of the high pressure gaseous systems under consideration in this report. Following these, the details relating to the use of a waveguide are discussed in two subsections:

Subsection 1a deals with the general application of a hollow waveguide, summarizing the past work relevant to the topics of this report.

Subsection 1b outlines the basic losses associated with propagation of radiation in different types of waveguides, including a discussion of losses when the waveguide is used as a part of a resonator.

Section 2 gives specific details of the gaseous systems suitable for optical pumping at a high pressure. This is discussed in two subsections:

Subsection 2a gives a summary of an optical pumping scheme in which a CO_2 gas is optically pumped at its 9.6 μ band, resulting in gain and hence laser oscillation on the 10.6 μ band. This system has been previously analyzed by Letokhov and his colleagues who have also made a demonstration of it in a pulsed device. The discussion gives the relevant parameters relating to CW operation. The extension of the method to N_2O molecules and the use of a mixture of several isotopic species are discussed.

Subsection 2b gives the details of a conceptually new approach in which the optically pumped high pressure gaseous system consists of a mixture of three primary gases, operating on the principles of energy storage and excitation transfer at an elevated vibrational temperature. This ternary gaseous system overcomes much of the difficulties of the previously known optically pumped energy transfer gaseous laser system which, due to these difficulties, require highly intense optical pumping radiation obtainable only in short duration pulses. It is shown in detail that, in the proposed ternary system, CW gains exceeding 0.01/cm can readily be obtained for 1 watt incident pump radiation coupled to an appropriate waveguide. In the example given, the pump radiation is obtained from a CW CO laser.

In collaboration with R.V. Hess and P. Brockman, NASA Langley, Hampton, Virginia, a computer modeling of the CO-NO system has been performed. This computer modeling estimates the transfer rates, the V-V and V-T decay rates for a large number of levels to account for the energy transfer through high-lying vibrational levels. The estimates of these rates are obtained via the prior-rate and surprisal analysis. A detailed knowledge of these rates

(and their temperature dependence) are of considerable importance in a variety of applications. These include detailed kinetic models of an e-beam CO laser and its analysis for room-temperature operation laser chemistry applications employing the CO molecules, and others.

Part II of this report summarizes the theoretical considerations in the computer model estimates of the V-V and V-T decay rates of CO-CO, CO-NO and NO-NO systems. It is shown that in high-lying vibrational levels, V-V decay rates for collisions with $\Delta v=2$ can become as large as the rates for collisions for $\Delta v=1$. This is a novel result which is of considerable importance in detailed estimates of the various transfer rates. Part II is concluded with a complete set of computer print-outs and graphs giving the decay rates for the CO-NO system up to $v=50$.

This is the final report for work performed during the period December 15, 1976 - December 17, 1977.

Subsection 1a - Hollow Waveguide for Optical Pumping

In free space, the laws of diffraction limits the distance over which a beam of light can propagate without an appreciable spread. Because of this, by reducing the beam diameter of an incident radiation with a lens or a telescope, large radiation power densities can only be produced over short propagation distances. The situation, however, can be drastically different if, instead of free space, propagation of light in a bound medium (i.e. a waveguide) is considered. In a hollow waveguide, the propagation of radiation via a low order - low loss waveguide mode can take place over relatively large distances without an appreciable reduction of the power density.

The use of an optical waveguide, in particular when filled with an active medium, has been exploited in a number of important applications - in fact, as is well known, the field of integrated optics is based on the concept of optical waveguides and their applications.

We will summarize below three recent applications in which a hollow waveguide filled with a gaseous medium is used at infrared wavelengths:

The first is the well known CO_2 waveguide laser in which a gaseous discharge through a hollow cylindrical dielectric waveguide containing a mixture of CO_2-N_2-He gases, excites the amplifying transitions of the CO_2 molecules. This in turn produces laser oscillations on the low loss electromagnetic mode of the dielectric waveguide used as a part of a high Q resonator.

The second consists of several far infrared metal waveguide lasers in which optical pumping with 10 μ CO_2 laser radiation is utilized to obtain far IR amplification and hence laser oscillation in a number of low pressure gases. As in CO_2 waveguide laser, the amplifying transitions are coupled to the low order - low loss waveguide

modes in a resonator. In these optically pumped devices, however, the 10 μ pump radiation is sufficiently intense for the optical pumping of the low pressure gases, so that its transmission through the far-IR waveguide, (which has a large diameter), takes place via multiple reflection off the waveguide walls, (without making use of the possibility of achieving enhanced pump radiation flux by coupling the pump radiation to a small area waveguide as discussed below).

The third is a recent series of experiments[1] in which a small diameter hollow waveguide filled with an absorbing gas is used to perform CW optical pumping with an incident radiation at 5 μ. In this case, the output of a CW CO laser is coupled to a low order-low loss waveguide mode, which allows propagation of incident radiation over appreciable distances at sizably enhanced radiation intensity flux needed for the optical pumping. In the experiments, NO molecules are used as the absorbing gas. The $v = 0 \rightarrow 1$ rotational-vibrational band of this molecule has a number of transitions which lie in close resonance with several of the strong oscillating CO laser lines. The use of the waveguide with a small cross sectional area made it possible to heavily saturate the absorbing NO transitions with the incident CO laser radiation tuned to the appropriate lines; this is achieved over an appreciable absorption path length (in excess of 70 cm). In this way, sizable population is produced in the $v = 1$ state of the NO molecule, making possible hot band absorption spectroscopy of this molecule's $v = 1 \rightarrow 2$ band. The hot band spectroscopy is performed by transmitting through the waveguide the radiation output of a CW frequency tunable spin-flip laser, as the saturating CW CO laser radiation is simultaneously coupled to the same waveguide.

In addition to the $v = 0 \rightarrow 1$ hot band spectroscopy, the use of the waveguide made it possible to observe

several coherent two quantum v = 0 → 2 transitions in the NO molecules--the observation of such a two quantum transition in absorption also requires intense incident radiation flux over an appreciable absorption path length in the gas sample.

This experiment has provided valuable information relating to the use of a small cross sectional area waveguide to obtain sizable population in an excited molecular vibrational level via CW optical pumping—this information supports many of the conclusions stated in this report.

Subsection 1b - Waveguide Losses

There are a number of recent publications[2,3,4,5,6] which treat the propagation modes in a hollow waveguide and the associated waveguide losses, as well as the losses when the waveguide is used in a resonator with external reflecting optics. We shall summarize here the results relevant to the purpose of this discussion.

We shall first discuss the losses associated with the lowest order propagating mode in the waveguide. Consider a hollow cylindrical dielectric waveguide. In this case, the lowest loss propagation mode is the hybrid EH_{11} mode. For a 1 mm diameter waveguide (corresponding to an area of $10^{-2}cm^2$), the EH_{11} losses (for a quartz waveguide) at 10 μ is 0.0013/cm. In this type of waveguide, the losses increase rapidly at reduced diameters: at 0.36 mm diameter, (corresponding to an area $10^{-3}cm^2$), the losses at 10 μ will be 0.04/cm.

Cylindrical metallic waveguides have lower losses. In this case, the lowest loss mode is the TE_{01} mode. In a copper cylindrical waveguide 360 μ in diameter, (corresponding to an area A = $10^{-3}cm^2$), the losses for 10 μ radiation is 0.0002/cm. For a 200 μ diameter (area 3 x $10^{-4}cm^2$) losses become 0.0015/cm and for 120 μ diameter (area = $10^{-4}cm^2$), the losses will be 0.007/cm.

The TE_{11} mode configuration, however, is doughnut shape with the E-field polarization at each point perpendicular to the doughnut radius passing through the point. Accordingly, case must be taken in using the output of a laser oscillating on this mode for application as a local oscillator in superheterodyne detection. For this, half of the output beam must be blocked — otherwise, because of a change in E-field polarization direction, there will be cancellation effect due to phase change in heterodyning.

Rectangular waveguides have some advantages, particularly for their tolerances against additional losses due to small curvatures along the waveguide length. Here we give the characteristics for a hybrid case in which two opposing waveguide walls are dielectric and the other two walls are metallic. In this case, for a waveguide 100 micron in thickness and one millimeter wide, (corresponding to an area of $10^{-3}cm^2$), the losses at 10 μ radiation is 0.002/cm. (This is for the case in which the wider dimension is the metallic wall and the thin dimension is the dielectric wall. The corresponding E-field polarization for the low loss mode is parallel to the metallic wall.)

In several examples given below, the total available CW pump powers are in the range of 1 to 10 watts. According to the above summary, the use of a waveguide with a cross sectional area of $10^{-3}cm^2$ will enable operation at pump power densities in the range of 1 to 10 kilowatt/cm^2.

Another consideration requiring attention is the overall losses when the waveguide is used as a part of a resonator. Two cases must be distinguished: the first is the case in which the reflecting optics for regenerative feedback consist of reflecting mirrors placed in direct contact with (or very close to) the waveguide ends. In this case, the situation is straightforward, since the overall losses will merely consist of the sum of the

waveguide propagation losses discussed above and the end mirrors' transmission losses.

The second is the case in which the waveguide is coupled to the free space and an external optical system, consisting of curved mirrors (or an equivalent system), provides the feedback. This problem has been extensively treated[3,4] particularly for the dielectric waveguide. In summary, the resonator mode inside the waveguide is expressed as a superposition of the propogating waveguide modes, and, in the region outside the waveguide, it is expanded in terms of the free space modes (of an open resonator) bounded by the reflecting optics. Across the cross section at either end of the waveguide, the field expression in the inside of the waveguide is matched to the field expression outside of it. The eigen states are then sought as the solutions which regenerate themselves after each round trip propagation in the resonator. Following this procedure, it is found that, with appropriate reflecting optics suitably placed at either ends, the low order resonator modes will correspond to a solution inside the waveguide consisting mainly of the low order - low loss waveguide modes with small admixture of the lossy higher order modes. Two situations are identified for which the losses of the lowest order mode of the overall resonator are at a minimum:

The first is the case where the separation of each curved mirror from the waveguide end closest to it is equal to its focal distance, the second is the case where this separation equals the mirror's radius of curvature. In both cases, the lowest loss is obtained when each mirror's curvature is taken to coincide with the curved wavefront of the appropriate open space propagation mode, having its beam waist at the waveguide end (and a cross sectional area at the beam waist properly matched to the waveguide inside dimensions). Estimate shows that,[3,4] for

instance, for a ten cm waveguide with 1 mm inside diameter, the single pass resonator losses can be as low as 1.5%.

The situation is expected to be considerably better for a resonator utilizing a circular or rectangular metallic waveguide (or a hybrid rectangular waveguide made of a pair of metallic and a pair of dielectric walls). This is due to the fact that the low order modes in these waveguides have losses considerably less than a dielectric waveguide of the same cross sectional area, hence, their admixtures describing a resonator mode will also correspond to a low loss mode.

It is to be noted that, with an amplifying medium of sufficient gain, laser oscillation automatically occurs on the lowest loss mode of the overall resonator. Accordingly, in an oscillating laser, the propagating field inside the waveguide is optimally matched to the propagating field outside of it.

Coupling an externally applied radiation to a waveguide (as is necessary for the pump radiation) is a different matter; it will require matching the wave front of the incident radiation to the waveguide's propagating low loss modes. This can become a demanding task if the aim is to obtain an optimum coupling. However, an optimum coupling to the waveguide is by no means a necessity for the pump radiation since, for instance, a 20 or 30 percent coupling loss can be made up by increasing the incident radiation by an amount equal to the coupling loss.

Section 2 - Gaseous Systems Suitable for CW Optical Pumping in a Waveguide

The available CW pump radiation sources dictate the choice of the gaseous media for the optical pumping systems proposed here. For practical reasons, we mainly confine our attention to the use of two types of CW laser pump

radiation sources: the CO_2 laser and the CO laser. Possible use of other pump radiation sources, including the HF CW laser and the parametrically produced radiation utilizing integrated optics, are briefly discussed at the end of this section.

Subsection 2a - CO_2 Laser as the Optical Pumping Source

Letokhov and his colleagues[7,8] have theoretically analyzed optical pumping of a high pressure CO_2 gas via the 9.6 μ absorption band, [the (001) → $(02^{O}0)$]. In this case, a CO_2 laser oscillating on this band is used for the optical pumping; gain (and hence laser oscillation) is obtained on the 10.6 μ band. The same group has reported experimental observation of the effect[7,8] using a relatively intense pulsed CO_2 laser pump radiation—14% conversion efficiency is obtained. The experimental observations agree with their theoretical predictions. We summarize below the relevant predictions relating to the CW optical pumping of this system.

The maximum obtainable gain, g_m, in this system is $g_m = \alpha[\exp(+\Delta E/kT)-1]$, where α is the absorption coefficient of the CO_2 at the 10.6 μ band (which is 1.56×10^{-3}/cm at room temperature), and ΔE is the 103 cm^{-1} energy separation between the (100) and $(02^{O}0)$ vibrational states, (the lower states of the 10.6 μ and 9.3 μ bands respectively). At 450 K, one obtains $g_m = 2.7 \times 10^{-3}$/cm.

As the pump radiation intensity is increased, the 10.6 μ absorption in the high pressure gas reduces to zero and switches to amplification. At a pressure of 100 torrs, the threshold pump radiation flux for the onset of the amplification is 2.8×10^{3} watts/cm^2. At one atmosphere pressure, this threshold intensity is increased to 1.6×10^{5} watts/cm^2.

Letokhov and colleagues have discussed the use of a hollow waveguide with 100 μ in diameter to obtain enhanced

radiation power flux. The discussion in Section 1 of this report shows that the expected waveguide losses at these diameters are somewhat large. For a waveguide with $10^{-3}cm^2$ cross sectional area, however, the waveguide losses can be sufficiently low. For such a waveguide, the estimated threshold input power at one atmosphere pressure will be 160 watts, while at 100 torrs pressure, this is reduced to 2.8 watts. At a pump power twice the threshold, the gain at a temperature of 450 K will be between $1 \times 10^{-3}/cm$ to $2 \times 10^{-3}/cm$.

Accordingly we note that at pressures of several atmospheres, the total pump radiation needed in in the range of several hundred watts. At several hundred torr pressure, however, the required pump power is reduced to tens of watts. In this lower pressure region, mixture of several isotopic species of the CO_2 gas molecules will extend the frequency tuning range over a broad region of interest. (See Section 3)

Inspection shows that this method can be extended to a different system consisting of optical pumping of the N_2O molecules, with a CW CO_2 pump laser oscillating on the same 9.6 μ band. We note that a number of strongly oscillating CO_2 lines in this band closely overlap several of the N_2O transitions belonging to its 9.6 μ $(02^{o}0) \rightarrow (100)$ absorption band. Furthermore, because of several compensating factors, the optical pumping of the N_2O molecules is found to behave similarly to the CO_2 molecules discussed above. An advantage of the use of N_2O is that, unlike CO_2, all the rotational states (including both even and odd J's) are allowed. As a result, the spacing between adjacent rotational-vibrational transitions are about a factor of 2.5 times less than the spacings of the CO_2 lines. The abundance of the lines, along with the possibility of operating with mixtures of several N_2O isotopic

species, makes the optical pumping of the N_2O molecules an attractive possibility for the consideration of this proposal. (See Section 3)

Subsection 2b - Optical Pumping with a CW CO Laser

With sufficient care, a highly reliable line tunable CW gaseous discharge CO laser can be constructed, with the capability of operating on any one of a large number of CO rotational-vibrational lines. Depending on the oscillating line, the output power ranges from hundreds of milliwatts to several watts. We note here that, several years ago, there were a number of technical problems which limited the performance realiability of a CW CO laser. These problems were mainly related to the gas handling and the CO discharge tube design and its electrodes. It is now possible to construct a CW CO laser capable of operating stably and reproducibly without deterioration of its performance over a long period of time. The following discussion gives an important application of a CW CO laser in a novel optical pumping system based on energy storage and excitation transfer principles.

This method utilizes a ternary gas mixture in which the incident pump radiation is absorbed by a first molecular constituent of the mixture -- a second molecular species in the mixture serves as a reservoir to store the energy initially absorbed by the first gas -- a third gas molecules, the lasing molecules, in equilibrium with the rest of the system, maintains inverted population and hence optical gain in suitable transitions. The transfer of energy from the absorbing molecules, through the energy storing gas, to the lasing molecules occurs via near resonant VV type collisional excitation transfer.

An important distinguishing feature of this ternary system is that the absorption of pump radiation occurs in

molecules which differ from the energy storing molecules. This makes it possible to increase the pressure of the energy storing molecules to a relatively high value, as the partial pressure of the absorbing gas is independently adjusted to give a suitable absorption length for the pump radiation; as is seen below, the conditions for energy storage and its transfer to the lasing molecules are most favorable at elevated pressures of the energy storing molecules (and at lower pressures of the energy absorbing molecules). We further note that, with the same energy absorbing and energy storing molecular system, optical gains at different wavelengths can be obtained by using different suitably chosen lasing gases in the mixture.

In Section 1, it was noted that a number of strong absorption lines in NO molecules originating from its $v = 0 \rightarrow 1$ rotational-vibrational band, fall in close coincidence with several strongly oscillating CO laser lines. The most favorable case is the P_9 (13) CO laser line which lies at 1884.32 cm^{-1} (corresponds to a wavelength of 5.30695 μ), and is 600 MHz below the peak of the absorbing NO line. The CW CO laser output power on this line is typically one watt.

In the ternary gas mixture, NO molecules will be used as the energy absorbing species. We choose the CO molecules for the energy storage, because of its exceptionally long V-T decay rate. In our detailed estimate, we shall consider the CO_2 molecules as the lasing gas. There are a host of other suitable lasing cases, which are mentioned below.

The first vibrational state of the NO molecule lies at 1904 cm^{-1}. The CO $v = 1$ state lies at 2170 cm^{-1}. The CO_2(001) state lies at 2349.4 cm^{-1}. Accordingly, we note that CO_2(001) state is 445 cm^{-1} higher than NO $v = 1$ state. This state, however, is only 179 cm^{-1} higher than the CO $v = 1$ state.

Before proceeding with the estimates, we summarize a typical result. It is shown below that at a pressure of 2.8 atmospheres of CO, 8.3 torrs of NO and 60 torrs of CO_2, CW optical gain of 0.01/cm can be obtained at the 10.6 μ band of CO_2. This is obtainable in a waveguide with $10^{-3}cm^2$ cross sectional area (corresponding to 357 μ in diameter) coupled to the 1 watt CO laser line mentioned above, (so that the pump radiation flux in the waveguide is 1 KW/cm). Under the conditions described, the absorption coefficient of the NO line is 0.04/cm, corresponding to 25 cm absorption length.

The following pages, summarize the estimates.

Estimate of gain

The estimate presented here is based on an approximate model describing the equilibrium distribution of population in the various vibrational states in terms of a vibrational temperature. Detailed inspection of a host of gas kinetic processes in the optically pumped ternary system verifies the validity of the model, as long as the gas kinetic temperature is not appreciably below the room temperature. (The proposed optical pumping will be done at a room temperature.)

To begin with, we give a number of relevant parameters of the gas molecules considered here.

The CO/CO VTR deactivation rate is 1.9×10^{-3}/sec/torr.

The NO/NO VTR deactivation rate is about 10^6 times higher and is 2.5×10^3/sec/torr.

NO/CO VV transfer rate is 652/sec/torr.

CO/CO VV transfer rate is close to the NO/NO rate and is 700/sec/torr.

CO_2/CO_2 deactivation rate for the (001) state is 3.35×10^2/sec/torr.

Collision broadening (FWHN) for CO_2 by CO is 6.5 MHz/torr.

The broadening of CO_2 by NO is 7.0 MHz/torr.

The NO self-broadening and its broadening by CO are not accurately known. We will adopt a typical value of 8 MHz/torr FWHM in our estimate.

Measured absorption coefficient of the NO line under consideration is 1/cm at one torr in pure NO, where the line width is due to Doppler broadening. (The measurement is done at MIT.)

As is seen below, under an optimum condition, the CO partial pressure is at several atmospheres, with the NO and CO_2 gas molecules at sizably lower partial pressures. Under this condition, the NO and CO_2 line broadenings are dominated by collisions with the CO molecules. Inspection shows that, in this case, the absorption coefficient, α, of the NO absorption line under consideration can be numerically written as:

$$\alpha = 10.7 \frac{p_n}{p_c} \quad ; \qquad (1)$$

where α is in reciprocal cm., p_n and p_c are the NO and CO gas pressures, respectively. The numerical factor in this equation is the products of all factors, including the Boltzman factor for the absorbing NO level, the square of the matrix element, etc. (This expression is obtained from

the measured absorption coefficient of NO and the line broadening coefficient of NO by CO given above.)

Let us assume an acceptable absorption coefficient, $\alpha = 0.04/cm$, corresponding to 25 absorption length. We shall impose this as a fixed condition throughout the calculations which follow. From this and expression (1), we will obtain:

$$\frac{p_c}{p_n} = 268 \qquad (2)$$

We shall further assume that the incident radiation flux at the 5.3 μ wavelength of the NO absorption line is 1 kw/cm^2. This will correspond to a rate, R, of the incident photon flux given by:

$$R = 2.7 \times 10^{22}/sec/cm^2.$$

For this incident radiation, the absorbed photons per second and per unit volume is:

$$\Delta R = \alpha R$$
$$= 1.1 \times 10^{21}/sec/cm^3.$$

ΔR represents the number of NO molecules making transitions to the v = 1 state per cm^3 and per sec.

The number density of molecules, n_1, in the NO v = 1 state will be given by $n_1 = (\Delta R)T$, where T is the V-T decay rate of the NO molecules, which is $T = 4 \times 10^{-4}/p_n$, with p_n expressed in torrs. From this, we will have:

$$n_1 = \frac{4.4 \times 10^{17}}{p_n}$$

It follows that the ratio of this n_1, to the density of NO molecules, n_o, in the ground vibrational state is given by:

$$\frac{n_1}{n_o} = \frac{13.8}{p_n^2}$$

This holds, as long as $\frac{n_1}{n_o} << 1$.

As an example, let us take $\frac{n_1}{n_o} = 0.2$,

in this case, $p_n = 8.3$ torrs. The CO pressure obtained from (2) will be $p_c = 2200$ torrs (which is 2.8 atmospheres). Accordingly, a mixture of 8.3 torrs NO and 2.8 atmospheres of CO will have an absorption length of 25 cm, (i.e., $\alpha = 0.04$), at the wavelength of the incident pump radiation tuned to the 5.3 μ NO absorption line. Furthermore, for 1 kw/cm^2 incident radiation flux, the NO v = 1 state will be populated according to $(n_1/n_o) = 0.2$, corresponding to a vibrational temperature of ~1700 K.

Let us for the moment consider a mixture of CO and NO gas (without CO_2). We note that, even in presence of several atmosphere CO pressure, the VT deactivation of NO is by far dominated by its own NO/NO self-deactivation process (as assumed above). The VV transfer rate between CO and NO, however, occurs at a rapid rate. This, on the average, does not effect the density of the NO vibrational state estimated from its self deactivation lifetime. This is because, in the steady state, the VV transfer from NO to CO is entirely balanced by its reverse process from CO to NO. This is true, as long as the VT decay of CO is very slow, which happens to be valid under the operating conditions described here.

Let us specifically consider the following energy transfer process:

$$NO(v = 1) + CO(v = 0) \underset{\Gamma_r}{\overset{\Gamma_f}{\rightleftarrows}} NO(v = 0) + CO(v = 1)$$

Γ_f and Γ_r are respectively the rates for the forward and the reverse processes as indicated. These are given by: $\Gamma_f = N_o\ \theta_f$ and $\Gamma_r = n_o\ \theta_r$, where n_o and N_o are the densities of the v = o states of the CO and NO molecules respectively and θ_f and θ_r are the averages of $\langle v\sigma \rangle$ over velocity distribution of the collision partners in the forward and the reverse processes respectively. (These quantities are related by $(\theta_f/\ \theta_r) = \exp[-\Delta E/kT]$ where ΔE is the vibrational energy of the CO minus the vibrational energy of NO, which is 164 cm^{-1}.)

Consider the 8.3 torrs NO and 2.8 atmospheres of CO gas mixture (corresponding to α = 0.04/cm). For these partial pressures we will have:

$$\begin{aligned} \Gamma_f &= 1.5 \times 10^6/\text{sec.} \\ \Gamma_r &= 6 \times 10^3/\text{sec.} \end{aligned} \qquad (3)$$

(These are obtained from the known NO/CO VV transfer rate of 652/sec/torr given above.)

If all other processes were to be ignored, in equilibrium we will have:

$$n_1\ \Gamma_f = N_1\ \Gamma_r; \qquad (4)$$

with n_1 and N_1 representing the densities of the v = 1 states of the CO and NO respectively. From (3) and (4), we observe that in equilibrium, $N_1 >> n_1$. This situation originates from the fact that CO pressure is much higher than NO, leading to $\Gamma_f >> \Gamma_r$ as indicated by (3), and despite a much larger CO pressure, the rate limiting VT decay still occurs through NO self deactivation.

The above analysis leaves out the effect of VV type collisions between two vibrationally excited molecules. Detailed inspection shows that this effect tends to distribute the excited molecules among the higher vibrational states, without appreciably affecting the total densities of the vibrationally excited molecules of either of the two molecular species. Furthermore, it can be shown that, at elevated gas temperatures where the VV energy defects are appreciably less than kT, the collisional processes tend to distribute the molecules over the various vibrational states according to a Boltzman distribution at a given temperature, with the CO vibrational temperature slightly below the NO vibrational temperature. Accordingly, the NO v = 1 state as well as the CO v = 1 state will have the highest populations compared to their respective populations in the v > 1 states.

This situation is approximately valid at room temperature. At a temperature around liquid N_2 temperature (or less), on the other hand, the collisional anharmonic pumping of the vibrationally excited CO molecules, as well as the NO-CO VV energy defect pumping, can become an appreciable effect. In that case, the populations of the excited vibrational states in both molecules tend to shift to their higher lying vibrational states. In fact, under appropriate conditions, an inverted population within the excited vibrational states of CO and NO molecules can occur at a low gas kinetic temperature.

(At this point, we note parenthetically that, in many respects, a CO molecule in a high lying vibrational state, plays a role similar to its v = 1 state. For instance, the VV CO/CO_2 excitation transfer process leading to production of the CO_2 in the (001) state considered below can take place as effectively for CO on a v > 1 state as for the CO v = 1 state. This is noted to show that a shift of population to high lying vibrational state in CO

does not appreciably alter the obtainable gain in CO_2; this further justifies our ignoring this effect in the estimate presented below.)

For reasons summarized above, we can safely proceed by assuming that at room temperature (or higher), the vibrational temperature of the CO v = 1 state raises to a value near the NO v = 1 vibrational temperature. From this it follows that:

$$\frac{n_1}{n_o} \cong \frac{N_1}{N_o}$$

where the ratio (n_1/n_o) is determined from the rate of incident photon absorption in NO and the NO VT decay lifetime (arising from its self deactivation), as per estimates given above.

From this, we conclude that, in our typical example of 8.3 torrs NO - 2.8 atmospheres CO, and an incident optical pumping radiation flux of $10^3 W/cm^2$, the equilibrium vibrational temperature of CO reaches a value close to the above 1700 K estimate of the NO vibrational temperature. From this we obtain the number of vibrationally excited CO molecules to be:

$$N_1 \approx 1.4 \times 10^{19}/cm^3$$

Before we proceed further, here we note that, in a recent experiment by Deutsch and Kildal[9], a mixture of CO_2-CO-He is optically pumped by a radiation pulse at a wavelength in close coincidence with the $P_1(14)$ line of the CO molecules. (This is done by harmonic generation starting from a pulsed CO_2 TEA laser.) Energy transfer from CO to CO_2 produces gain and hence laser oscillation on the 10.6 μ band of CO_2. In optimum situation, laser oscillation is obtained with 2 milli joule incident 5 micron radiation in a 200 nanosecond pulse, with a 4.3 cm length for the optically pumped medium producing the gain. This

is done with an incident radiation having a cross sectional area of 0.1 cm^2. If we assume that at least 50% of the incident pump photons are absorbed over the 4.3 cm length of the sample, then, the total number of the CO molecules excited into its v = 1 state over the 200 nanosecond pulse widths will be 50% of the total photons, in the 2 mj incident pump radiation. This will correspond to 10^{16} total excited molecules. Dividing this by the volume of the sample, we obtain a density of $N_1 = 2 \times 10^{16}/cm^3$. The data presented by Deutsch and Kildal does not give the partial pressures of the gases at which the 2 mj threshold pump radiation is observed. A detailed inspection of their data shows the likelihood that their incident 2 mj minimum threshold pump radiation may have been absorbed over 0.5 cm length of their gas sample. In this case, their excited CO density at the most will be $N_1 = 2 \times 10^{17}$.

This is noted in support of the potentials of this optical pumping method: in our case, we can maintain considerably higher density of the vibrationally excited CO molecules in a CW fashion, as compared to the density produced in their transient pulse of 200 nanosecond in duration.

Let us now continue by introducing CO_2 in the NO-CO gas mixture. In this system, the dominant source of CO_2(001) excitation is the near resonant VV transfer via CO/CO_2 collisions. Detailed inspection shows that, at a low CO_2 VT self deactivation (of its 001 state) occurs at a rate slower than the VV transfer from its (001) state back to the CO molecules, the vibrational temperature of the CO_2(001) molecules will be closely the same as that of the CO and NO vibrational states. We further note that the CO_2 partial pressure can be safely increased until its VT self deactivation becomes comparable to the NO VT deactivation. At a higher CO_2 pressure, however, the self deactivation of CO_2 becomes the decay limiting rate, causing a decrease of the overall vibrational temperature of the gas mixture.

The VT decay rate of NO at 8.3 torrs partial pressure is 2.1×10^4/sec. At a partial pressure of 60 torrs of the CO_2 gas, the $CO_2(001)$ VT decay rate (arising from its self deactivation) becomes comparable to the NO VT self deactivation rate. We further note that, at the 2.8 atmospheres CO partial pressure considered here, the VV transfer rate from $CO_2(001)$ state back to CO, occurs at a rate of 1.5×10^6. This is about two orders of magnitude higher than the VT self deactivation rate of $CO_2(001)$ state (at 60 torrs of CO_2 partial pressure). This is an important criterion, which dictates that the equilibrium vibrational temperature of the (001) state is closely the same as the CO vibrational temperature. The rate of $CO_2(001)$ VV transfer to NO, however, is only 830/sec. which is appreciably below its VT self deactivation rate. This shows the importance of the role played by CO: Without the presence of a high CO partial pressure, the $CO_2(001)$ vibrational temperature cannot reach the equilibrium vibrational temperature of the NO v = 1 state.

From the above, it follows that in equilibrium, the number density, m, of the $CO_2(001)$ molecules in the optically pumped mixture considered, will be

$$m = 3.8 \times 10^{17}/cm^3.$$

Specifically, this is obtained for CO-NO-CO_2 mixture at partial pressures of 2.8 atmospheres - 60 torrs - 8.3 torrs respectively, and for an incident pump radiation flux of $10^3 W/cm^2$ at a wavelength of the NO absorbing line.

Detailed inspection of the gain expression in the 10.6 μ of CO_2 shows that, for the P (20) line we can write numerically:

$$g = 1.1 \times 10^{-9} \ (m\tau)$$

where g is the gain value per cm, m is density of CO_2 molecules in the (001) vibrational state and τ is given by

$\Delta\nu = 1/2\pi\tau$ where $\Delta\nu$ is the collision broadened half width of the P (20) line. The rotational Boltzman factor, matrix element square, and all other factors are lumped in the numerical coefficient. (In this expression, the lower level population of the 10.6 μ band is assumed to be sufficiently below the upper level population and, hence, it is ignored.)

For a (FWHM) of 6.5 MHz/torr collisional line width broadening of CO_2 by CO, and for a number density of CO_2 (001) given by the above value of $m = 3.8 \times 10^{17}/cm^3$, we obtain:

$$g = 0.01/cm$$

In our above estimate, we have avoided giving detailed expressions for the lengthy coupled rate equations. All the arguments for the validity of the model presented above is based on term-by-term inspection of the coupled rate equation. More detailed calculations, including the effect of VV collisions between the vibrationally excited molecules, will have to be performed with kinetic modeling computer calculations. The results obtained, however, warrants conducting an experimental program to show the possible existence of the gain and the prediction of laser oscillation.

REFERENCES

1. M. Guerra, A. Sanchez, and A. Javan, Physical Review Letters, Vol. 38, No. 9, 28 Feb., 1977.

2. E. A. J. Marcatili and R. A. Schmeltzer, Bell Syst. Tech. J. 43, 1783 (1964).

3. A. N. Chester and R. L. Abrams, Appl. Phys. Lett. 21, 576 (1972).

4. R. L. Abrams, IEEE J. of Quantum Electronics Q.E. - 8, 838 (1972).

5. P. W. Smith, Appl. Phys. Lett. 19, 132 (1971). See also, R. L. Abrams and W. B. Bridges, IEEE J. of Quantum Electronics Q.E. - 9, 940 (1973).

6. E. Garmire, T. McMahon, and M. Bass, Appl. Phys. Lett. 15, 145 (1976).

7. A. L. Gager and V. S. Letokhov, Sov. J. Quant. Electron., 5, 811 (1975).

8. V. I. Balykin et al., Sov. J. Quant. Electron., 4, 1325 (1975).

9. H. Kildal and T. F. Deutsch, App. Phys. Lett. 27, 500 (1975). See also: Same authors. Proceedings of the 9th Quantum Electronics Conference, Amsterdam, 1976. For an earlier work see: T. Y. Chang and O. R. Wood, Appl. Phys. Lett. 24, 182 (1974).

Part II - Estimates of V-V and V-T Rate Constants in Pure CO and NO Gases and CO-NO Gas Mixtures

The surprisal analysis developed by R.D. Levine et al.[1] is used to predict the V-V and V-T transition rates for vibrational levels up to v = 50 for collisions involving combinations of the species CO and NO.

The surprisal analysis developed by Levine and his coworkers is based on the assumption that the rate constants for vibrational energy transfer can be written in the form[2]:

$$k(v \to v') = A(T) k^{o}(v \to v';T) \exp[-\lambda_v |E_v - E_{v'}|/kT] \quad (1)$$

A(T) depends on temperature alone and in the terminology of the theory $k^{o}(v \to v';T)$ is called the prior rate while λ_v is a measure of the surprisal (discussed below), the difference between the actual and the prior rate. As in reference 2, λ_v is a shorthand notation for λ vibration; no other significance should be deduced for subscript in λ_v.

The prior rates are calculated from a statistical approach to the dynamics in which all final states allowed by the available energy are considered equally probable. The analysis of the prior transition rate is given in the paper by Procacia and Levine[2]. In particular, for diatomic-diatomic collisions they find:

$$k^{o}(v,m \to v',m';T) = [R(\tfrac{32}{15}) A_T (kT)^{2.5} \pi^{-1/2}] \Delta^3 \exp[\Delta] K_3(\Delta) \quad (2)$$

where:

v, m; v', m' are the initial and final vibrational states of the molecules involved

$$\Delta = (E_v + E_m - E_{v'} - E_{m'})/2kT$$

$$A_T = (\mu)^{3/2} \, 2^{1/2} \, (\Pi)^2 \, (\hbar)^3$$

μ = reduced mass of collision partners

R = proportionality constant independent of the energy

$K_3(\Delta)$ = third order modified Bessel function of the second kind

Substituting equation 2 into equation 1 [expressed for initial and final states indicated by (v, m; v', m')], yields for diatomic-diatomic collisions an equation for the transition rate of:

(3)

$$k(v,m;v',m',T) = C(T)\Delta^3 \exp(\Delta)K_3(\Delta) \exp\left[-\lambda_v|2\Delta|/kT\right]$$

where two unknowns, C(T) and λ_v, are left to be determined. If experimental values are available for rates involving the molecules being studied then matching the rate to two experimental points will specify the unknowns. If no experimental results are available, then various sum rules can be used to "synthesize" the necessary parameters. This approach is detailed in Procacia and Levine[2]. Since experimental measurements are available for all the combinations of molecular species involved in this study, we will not deal with this synthetic approach to the problem.

While in principle any two experimentally available points are adequate, it is advantageous if at least one V-T transition is available. Since λ_v determines the exponential dependence of the rate on the energy defect, it is important that one obtains an accurate value for λ_v. If the experimental points being matched are all V-V, which have relatively small energy defects, then they are not a very sensitive determinant of λ_v. Slight shifts in λ_v which optimize the fit to V-V values available could lead to drastic errors in predicting V-T rates with large

energy defects. Therefore in this work values for λ_v and C(T) were chosen so as to best fit both V-V and V-T experimentally available points.

The "surprisal" is defined as

$$I(v, v';T) = \ell n\left[\frac{k^{o}(v \rightarrow v';T)}{k\ (v \rightarrow v';T)}\right] \qquad (4)$$

Here we consider, for example, a V-T decay in which $E_m = E_{m'}$ (hence E_m is not explicitly indicated). Thus, λ_v is a direct measure of the difference between the prior rate and the actual rates as found experimentally. If $\lambda_v = 0$, it means that all final states with a certain energy are equally probable. When $\lambda_v > 0$, it is more probable that the final state will be close to the initial state in vibrational level. That is, as λ_v increases positively in size, it becomes less and less likely that the energy available in a collision will be redistributed. A width of kT/λ_v can be used as a guideline for determining which transitions are probable. For transitions to be probable their energy defect should be less than this width. A negative λ_v would imply that the final states would be unlikely to be near the initial state. All the λ_v's encountered here were found to be positive.

The determination of λ_v and C(T) first involves calculation of the prior rates as given in equation 2. At this stage R is still undetermined so k^o/R is calculated instead of k^o. This value is then substituted for k^o in the equation for k and is equivalent to incorporating the unknown R into C(T) which is still to be determined.

It is most efficient to first calculate k^o for two transitions where values are experimentally available. Then using these rates to determine λ_v and C(T) it becomes immediately obvious which transitions will be so unlikely to be negligible. For instance, with large positive λ_v any transition with a large energy defect becomes improbable.

Thus V-V transitions with $\Delta V>1$ and any V-T types of transitions would have rates small compared to other processes with smaller defects. If one plots the surprisal I on the ordinate axis and $|\Delta E/kT|$ on the abscissa then one obtains a straight line whose slope is λ_v (dimensionless). We have extensively investigated fitting such a plot to the experimental data of references 3 through 13 (discussed below) to obtain the surprisal parameters for CO-CO, NO-NO, and CO-N) collisions. (Once λ_v is determined then equation 3 for k is used and C(T) calculated so that the predicted value matches the corresponding experimental value.) With λ and C values set an exact equation is written for the transition rate k. The rate is expressed in terms of the energy defect. From this work the following equations are found for the transition rates involving collisions between combinations of molecules of CO and NO:

T = 298 K

CO-CO

$$k = (1.15 \times 10^4) e^{-2.10|2\Delta|} \Delta^3 K_3(\Delta) e^{\Delta}$$

NO-NO

$$k = (1.42 \times 10^4) e^{-.737|2\Delta|} \Delta^3 K_3(\Delta) e^{\Delta}$$

NO-CO

$$k = (2.41 \times 10^5) e^{-6.50|2\Delta|} \Delta^3 K_3(\Delta) e^{\Delta}$$

all the transition rates are in ($torr^{-1}$ sec^{-1}), and are determined for room temperature. The experimental values used for CO-CO are obtained from references 3 through 9. For the NO-NO calculations the experimental values are those of G. Salvetat et al.[10], Nachshon and Coleman[11], and J.C. Stephenson[12]. For the NO-CO relaxation rates the

experimental values in references 3 and 12 through 14 are used to determine λ_v and C(T).

The theory agrees well with the available experimental points for CO-CO and NO-NO collisions. A good fit can also be made for all the available V-V rates in CO-NO types of collisions. This includes the V-V rate of Weeks and Yardley[14]. However, the V-T rate in that work differs drastically from that predicted by surprisal analysis using the V-V experimental points. Any attempt to fit that point to the theory leads to large discrepancies between the predicted V-V rates and those measured by several authors. In some cases more than one author has measured the same V-V rate and they are in agreement as to its value. Weeks and Yardley used a laser excited fluorescence technique to measure their rates, and the authors themselves point out that their errors could be high. Thus we are forced to ignore this one isolated point. As this was the only V-T rate available, it means the predicted V-T rates could still be well off from the actual rates since we have no sensitive way of determining λ_v. However, in any case, these rates will be small and should have only a small effect on the populations determined by the master equation.

Note the large λ's for both CO-CO and NO-NO types of collisions. Since at room temperature kT=200 cm^{-1} any collisional transfer with an energy defect greater than ~50-100 cm^{-1} (kT/λ) becomes increasingly unlikely for these molecules. The collisional energy transfer of most interest to us in this study of that of the NO-CO type where

$$NO(v=1) + CO(v=0) \rightarrow NO(v=0) + CO(v=1) - 267\ cm^{-1}$$

With the energy defect so much larger than kT/λ it will require many collisions of an excited NO molecule with a ground state CO molecule before a transfer will take place.

The case of

$$CO(v) + NO(v') \rightarrow CO(v+1) + NO(v'-1) + \Delta E$$

is presented in Figure 1. The logarithm of the rate in units of $torr^{-1}$ sec^{-1} is plotted versus v for constant v'. The rate for a particular v' reaches its peak versus v when the energy defect changes in sign. There is a cyclical nature to the magnitude of the peaks of these collision rates. The molecules of NO and CO have slightly different vibrational energy level spacings, thus the minimum energy defect for collisional transfers will in general never be zero. However it will increase and decrease in a periodic way as the energy levels for NO and CO come into near coincidence and then move apart again. It's similar to the beating between two approximately equal frequencies where the envelope of the beat has a periodicity determined by the difference in frequencies.

Although on either side of the break the curves of Fig. 1 appear to be straight lines, they are not. There is a curvature downward to the left of the break and a curvature upward on the right. However, the nearness to perfectly straight lines on a log plot implies that collisional transfers of this type can be approximately represented by a simple scaling law. From the plot one finds

$$\text{NO-CO} \qquad k(v,v';\ 290\ K) \triangleq \begin{cases} k(v=0,v')(e^{.89v}) & \text{up to quasi-resonance } (v_r \triangleq v'+9) \\ k_r e^{-.71(v-v_r)} & \text{where } k_r \text{ is } k \text{ calculated at } v_r \end{cases}$$

where k_r and v_r refer to the rate and the v at the peak of that particular v' plot. The subscript r is used here to indicate a quasi-resonance behavior appearing in the form of a peak of the v' plot.

A similar relationship can be written for V-T rates. Table I lists the rates for collisions of the type

$$CO(v+1) + NO(v') \rightarrow CO(v) + NO(v') + \Delta E$$

From this data one finds

$V\text{-}T_{CO\text{-}NO}$

$$k(v+1\rightarrow v) \triangleq e^{.79(v)} k(1\rightarrow 0)$$

Scaling laws like these can be derived for all the types of collisions considered here. For a V-T type of collision involving two molecules

$$CO(v+1) + CO(v') \rightarrow CO(v) + CO(v')$$

Table II has the rates for the first ten vibrational levels. This yields the following relationship:

$V\text{-}T_{CO\text{-}CO}$

$$k(v+1,v) \triangleq e^{2.5v} k(1\rightarrow 0)$$

which is similar to the V-T rate above. However, note that $k(1\rightarrow 0)$ for a collision between two CO molecules is more than eighteen orders of magnitude as likely to result in a V-T decay than that collision between a CO molecule and an NO molecule. Therefore, for comparable pressures, NO-CO collisions can be neglected as a channel for V-T decay in CO.

Fig. 2 is a plot of CO-CO vibrational transfer rates. Once again the nearly perfect straight lines on the semi-log plot can be represented by

$V\text{-}V_{CO\text{-}CO}$

$$k(v,v';T) \triangleq \begin{cases} k(v=0,v';T)e^{.33(v)} & \text{up to } v_r=v'-1 \\ k(v=v_r;\ v';T)e^{-20(v-v_r)} \end{cases}$$

where $k(v, v'; T)$ is the rate for a collisional transfer of the type

$$CO(v) + CO(v') \rightarrow CO(v+1) + CO(v'-1)$$

For NO-NO collisions the same general relationships hold true. NO is the only stable diatomic molecule with a non zero electronic angular momentum. Because of this its energy levels are doubled. It has two electronic ground states $^2\pi_{1/2}$ and $^2\pi_{3/2}$. The $^2\pi_{3/2}$ level is 123 cm^{-1} above the $^2\pi_{1/2}$ level. These two levels are thermalized by spin relaxation on a tens of nanoseconds time scale. Bauer and Sahm[15] measured that about 70 collisions are required to equilibrate these electronic levels. Thus, the populations of these levels are tied together and one set of rate equations can be used for the vibrational levels. Fig. 3 is a plot of the NO-NO vibrational transfer rates for a collision of the type

$$NO(v) + NO(v') \rightarrow NO(v+1) + NO(v'-1)$$

Again these rates can be approximately represented in the form

$$k(v,v';T) \triangleq \begin{cases} k(v=0,v')e^{.17v} & \text{up to resonance } (v_r=v'-1) \\ k(v=v_r,v')e^{-.04(v-v_r)} & \end{cases}^{V-V_{NO-NO}}$$

Note that all of the rates plotted so far, those of NO are the most curved. However, the above approximation still gives reasonably accurate values. For instance, worst case examples are within a factor of 2 of the actual calculated rates. To complete this set of scaling laws, the V-T rates for NO-NO collisions of the type

$$NO(v+1) + NO \rightarrow NO(v) + NO$$

are listed in Table III. These values can be represented by

$$V\text{-}T_{NO\text{-}NO} \qquad k(v+1\rightarrow v) \cong e^{.07v} k(1\rightarrow 0)$$

Once again the scaling factor is on the order unity as in the other V-T cases but note how much larger $k(1\rightarrow 0)$ is for NO-NO than it is for either CO-NO or CO-CO.

Of course all the rates presented here are temperature dependent. Theoretically λ_v is directly proportional to T as long as the temperature is low, that is, when h c w/kT>1. Otherwise, at higher temperatures λ_v is independent of T. The scaling factor C(T) also has a temperature dependence. Work has been done and is continuing on analyzing these rates at temperatures other than room temperature.

In conclusion, we state that in this work we have obtained a complete set of V-V and V-T rates (up to v=50 levels) for CO-CO, NO-CO, and NO-NO collisions. In addition to a variety of applications, these rates are needed for a detailed computer modeling estimates of vibrational equilibration in a CO-NO gas mixture subjected to an optical pumping excitation (or possibly, a discharge excitation). Such detailed estimates must include collisions between two vibrationally excited species, since such species will be heavily populated (due to the anharmonic collisional pumping effect). Such a computer modeling can be applied to the energy-transfer high pressure gas laser system described in Part I of this report, to obtain a detailed estimate of gain versus partial pressures of the various gas-mixture species and at varying optical pumping intensity.

The preliminary computer estimates using the rate equation for 50 vibrational levels of NO and CO (in which the above calculated V-V and V-T transfer rates are employed) have been conducted. The results are in general agreement with the conclusions described in Part I of this report. Further work, however, is required to complete the work.

The collision transfer V-V and V-T decay rates given in this report are of considerable importance for a complete computer modeling of an e-beam excited CO laser. The previous work has yielded contradictory results, mainly because of inaccurate estimates of the V-V and V-T decay rates. We believe that the calculated values presented in this report will resolve the uncertain status of the previous estimates.

REFERENCES

1. R.D. Levine and R.B. Bernstein, Acc. Chem. Res. 7, 393 (1974).

2. I. Procacia and R.D.Levine, J. Chem. Phys. 63, 4261 (1975).

3. G. Hancock and I.W.M. Smith, Appl. Opt. 10, 1827 (1971).

4. H.T. Powell, J. Chem, Phys. 59, 4937 (1973).

6. M.G. Ferguson and A.W. Read, Trans. Faraday Soc. 61, 1559 (1965).

7. M.A. Kovacs and M.E. Mack, Appl. Phys. Lett. 20, 487 (1972).

8. P.B. Sackett et al, Appl. Phys. Lett. 22, 367 (1973).

9. C. Wittig and I.W.M. Smith, Chem. Phys. Lett. 16, 292 (1972).

10. G. Salvetat and M. Clerc, J. Chem. Phys. (France) 71, 1053 (1974).

11. Y. Nachshon and P. Coleman, J. Chem. Phys. 61, 2520 (1974).

12. J.C. Stephenson, J. Chem. Phys. 59, 1523 (1973).

13. W.H. Green and J.K. Hancock, J. Chem. Phys. 59, 4326 (1973).

14. G.P. Weeks and J.T. Yardley, J. Chem. Phys. 61, 2163 (1974).

15. H.J. Bauer and K.F. Sahm, J. Chem. Phys. 42, 3400 (1965).

TABLE I VIBRATIONAL-TRANSLATIONAL RATES
IN NO-CO MIXTURE

INPUT 2 MOLECULES				VT rates for NO-CO	
NO	CO	NO	CO		
0	1	0	0	.1035E+02	.2329E-21
0	2	0	1	.1023E+02	.5255E-21
0	3	0	2	.1010E+02	.1179E-20
0	4	0	3	.9971E+01	.2630E-20
0	5	0	4	.9845E+01	.5832E-20
0	6	0	5	.9719E+01	.1286E-19
0	7	0	6	.9595E+01	.2818E-19
0	8	0	7	.9472E+01	.6141E-19
0	9	0	8	.9349E+01	.1330E-18
0	10	0	9	.9228E+01	.2865E-18
0	11	0	10	.9107E+01	.6135E-18
0	12	0	11	.8987E+01	.1306E-17
0	13	0	12	.8868E+01	.2764E-17
0	14	0	13	.8750E+01	.5815E-17
0	15	0	14	.8633E+01	.1216E-16
0	16	0	15	.8517E+01	.2530E-16
0	17	0	16	.8402E+01	.5230E-16
0	18	0	17	.8287E+01	.1075E-15
0	19	0	18	.8174E+01	.2197E-15
0	20	0	19	.8061E+01	.4464E-15
0	21	0	20	.7949E+01	.9017E-15
0	22	0	21	.7839E+01	.1811E-14
0	23	0	22	.7729E+01	.3615E-14
0	24	0	23	.7619E+01	.7176E-14
0	25	0	24	.7511E+01	.1416E-13
0	26	0	25	.7404E+01	.2778E-13
0	27	0	26	.7298E+01	.5419E-13
0	28	0	27	.7192E+01	.1051E-12
0	29	0	28	.7088E+01	.2026E-12
0	30	0	29	.6984E+01	.3884E-12
0	31	0	30	.6881E+01	.7402E-12
0	32	0	31	.6779E+01	.1403E-11
0	33	0	32	.6678E+01	.2642E-11
0	34	0	33	.6578E+01	.4948E-11
0	35	0	34	.6479E+01	.9213E-11
0	36	0	35	.6380E+01	.1706E-10
0	37	0	36	.6283E+01	.3139E-10
0	38	0	37	.6186E+01	.5745E-10
0	39	0	38	.6091E+01	.1045E-09
0	40	0	39	.5996E+01	.1891E-09
0	41	0	40	.5902E+01	.3400E-09
0	42	0	41	.5809E+01	.6079E-09
0	43	0	42	.5717E+01	.1081E-08
0	44	0	43	.5626E+01	.1910E-08
0	45	0	44	.5535E+01	.3357E-08
0	46	0	45	.5446E+01	.5865E-08
0	47	0	46	.5357E+01	.1019E-07
0	48	0	47	.5270E+01	.1760E-07
0	49	0	48	.5183E+01	.3022E-07
0	50	0	49	.5097E+01	.5159E-07

TABLE I Concluded

INPUT 2 MOLECULES VT rates for NO-CO

NO	CO	NO	CO		
1	0	0	0	.9063E+01	.8115E-18
2	0	1	0	.8927E+01	.1909E-17
3	0	2	0	.8791E+01	.4488E-17
4	0	3	0	.8656E+01	.1055E-16
5	0	4	0	.8520E+01	.2482E-16
6	0	5	0	.8384E+01	.5835E-16
7	0	6	0	.8249E+01	.1372E-15
8	0	7	0	.8113E+01	.3225E-15
9	0	8	0	.7977E+01	.7582E-15
10	0	9	0	.7841E+01	.1782E-14
11	0	10	0	.7705E+01	.4188E-14
12	0	11	0	.7569E+01	.9843E-14
13	0	12	0	.7433E+01	.2313E-13
14	0	13	0	.7297E+01	.5434E-13
15	0	14	0	.7161E+01	.1277E-12
16	0	15	0	.7025E+01	.2998E-12
17	0	16	0	.6889E+01	.7042E-12
18	0	17	0	.6753E+01	.1654E-11
19	0	18	0	.6617E+01	.3882E-11
20	0	19	0	.6480E+01	.9113E-11
21	0	20	0	.6344E+01	.2139E-10
22	0	21	0	.6208E+01	.5019E-10
23	0	22	0	.6071E+01	.1177E-09
24	0	23	0	.5935E+01	.2762E-09
25	0	24	0	.5799E+01	.6477E-09
26	0	25	0	.5662E+01	.1518E-08
27	0	26	0	.5526E+01	.3559E-08
28	0	27	0	.5389E+01	.8341E-08
29	0	28	0	.5253E+01	.1954E-07
30	0	29	0	.5116E+01	.4577E-07
31	0	30	0	.4980E+01	.1072E-06
32	0	31	0	.4843E+01	.2508E-06
33	0	32	0	.4706E+01	.5870E-06
34	0	33	0	.4570E+01	.1373E-05
35	0	34	0	.4433E+01	.3211E-05
36	0	35	0	.4296E+01	.7505E-05
37	0	36	0	.4159E+01	.1754E-04
38	0	37	0	.4022E+01	.4096E-04
39	0	38	0	.3885E+01	.9565E-04
40	0	39	0	.3749E+01	.2232E-03
41	0	40	0	.3612E+01	.5207E-03
42	0	41	0	.3475E+01	.1214E-02
43	0	42	0	.3338E+01	.2830E-02
44	0	43	0	.3200E+01	.6592E-02
45	0	44	0	.3063E+01	.1535E-01
46	0	45	0	.2926E+01	.3572E-01
47	0	46	0	.2789E+01	.8306E-01
48	0	47	0	.2652E+01	.1931E+00
49	0	48	0	.2515E+01	.4485E+00
50	0	49	0	.2377E+01	.1041E+01

TABLE II VIBRATIONAL-TRANSLATIONAL RATES IN CO-CO MIXTURE

INPUT 2 MOLECULES VT rates for CO-CO

CO	CO	CO	CO		
1	0	0	0	.1035E+02	.3792E-03
2	0	1	0	.1023E+02	.3700E-03
3	0	2	0	.1010E+02	.1112E-02
4	0	3	0	.9971E+01	.1419E-02
5	0	4	0	.9845E+01	.1808E-02
6	0	5	0	.9719E+01	.2298E-02
7	0	6	0	.9595E+01	.2915E-02
8	0	7	0	.9472E+01	.3692E-02
9	0	8	0	.9349E+01	.4666E-02
10	0	9	0	.9228E+01	.5886E-02
11	0	10	0	.9107E+01	.7411E-02
12	0	11	0	.8987E+01	.9314E-02
13	0	12	0	.8868E+01	.1168E-01
14	0	13	0	.8750E+01	.1462E-01
15	0	14	0	.8633E+01	.1827E-01
16	0	15	0	.8517E+01	.2279E-01
17	0	16	0	.8402E+01	.2837E-01
18	0	17	0	.8287E+01	.3524E-01
19	0	18	0	.8174E+01	.4370E-01
20	0	19	0	.8061E+01	.5409E-01
21	0	20	0	.7949E+01	.6682E-01
22	0	21	0	.7839E+01	.8239E-01
23	0	22	0	.7729E+01	.1014E+00
24	0	23	0	.7619E+01	.1245E+00
25	0	24	0	.7511E+01	.1527E+00
26	0	25	0	.7404E+01	.1869E+00
27	0	26	0	.7298E+01	.2282E+00
28	0	27	0	.7192E+01	.2782E+00
29	0	28	0	.7088E+01	.3385E+00
30	0	29	0	.6984E+01	.4112E+00
31	0	30	0	.6881E+01	.4984E+00
32	0	31	0	.6779E+01	.6031E+00
33	0	32	0	.6678E+01	.7283E+00
34	0	33	0	.6578E+01	.8779E+00
35	0	34	0	.6479E+01	.1056E+01
36	0	35	0	.6380E+01	.1268E+01
37	0	36	0	.6283E+01	.1521E+01
38	0	37	0	.6186E+01	.1819E+01
39	0	38	0	.6091E+01	.2172E+01
40	0	39	0	.5996E+01	.2590E+01
41	0	40	0	.5902E+01	.3081E+01
42	0	41	0	.5809E+01	.3659E+01
43	0	42	0	.5717E+01	.4337E+01
44	0	43	0	.5626E+01	.5132E+01
45	0	44	0	.5535E+01	.6060E+01
46	0	45	0	.5446E+01	.7144E+01
47	0	46	0	.5357E+01	.8406E+01
48	0	47	0	.5270E+01	.9872E+01
49	0	48	0	.5183E+01	.1157E+02
50	0	49	0	.5097E+01	.1354E+02

TABLE III VIBRATIONAL-TRANSLATIONAL RATES
IN NO-NO MIXTURE

INPUT 2 MOLECULES VT rates for NO-NO

NO	NO	NO	NO		
1	0	0	0	.9063E+01	.2306E+04
2	0	1	0	.8927E+01	.2482E+04
3	0	2	0	.8791E+01	.2672E+04
4	0	3	0	.8656E+01	.2876E+04
5	0	4	0	.8520E+01	.3092E+04
6	0	5	0	.8384E+01	.3325E+04
7	0	6	0	.8249E+01	.3575E+04
8	0	7	0	.8113E+01	.3842E+04
9	0	8	0	.7977E+01	.4128E+04
10	0	9	0	.7841E+01	.4435E+04
11	0	10	0	.7705E+01	.4762E+04
12	0	11	0	.7569E+01	.5112E+04
13	0	12	0	.7433E+01	.5487E+04
14	0	13	0	.7297E+01	.5886E+04
15	0	14	0	.7161E+01	.6313E+04
16	0	15	0	.7025E+01	.6768E+04
17	0	16	0	.6889E+01	.7254E+04
18	0	17	0	.6753E+01	.7772E+04
19	0	18	0	.6617E+01	.8324E+04
20	0	19	0	.6480E+01	.8912E+04
21	0	20	0	.6344E+01	.9537E+04
22	0	21	0	.6208E+01	.1020E+05
23	0	22	0	.6071E+01	.1091E+05
24	0	23	0	.5935E+01	.1166E+05
25	0	24	0	.5799E+01	.1246E+05
26	0	25	0	.5662E+01	.1331E+05
27	0	26	0	.5526E+01	.1421E+05
28	0	27	0	.5389E+01	.1516E+05
29	0	28	0	.5253E+01	.1617E+05
30	0	29	0	.5116E+01	.1724E+05
31	0	30	0	.4980E+01	.1837E+05
32	0	31	0	.4843E+01	.1956E+05
33	0	32	0	.4706E+01	.2082E+05
34	0	33	0	.4570E+01	.2215E+05
35	0	34	0	.4433E+01	.2356E+05
36	0	35	0	.4296E+01	.2503E+05
37	0	36	0	.4159E+01	.2659E+05
38	0	37	0	.4022E+01	.2822E+05
39	0	38	0	.3885E+01	.2994E+05
40	0	39	0	.3749E+01	.3174E+05
41	0	40	0	.3612E+01	.3363E+05
42	0	41	0	.3475E+01	.3561E+05
43	0	42	0	.3338E+01	.3768E+05
44	0	43	0	.3200E+01	.3984E+05
45	0	44	0	.3063E+01	.4209E+05
46	0	45	0	.2926E+01	.4444E+05
47	0	46	0	.2789E+01	.4688E+05
48	0	47	0	.2652E+01	.4942E+05
49	0	48	0	.2515E+01	.5206E+05
50	0	49	0	.2377E+01	.5479E+05

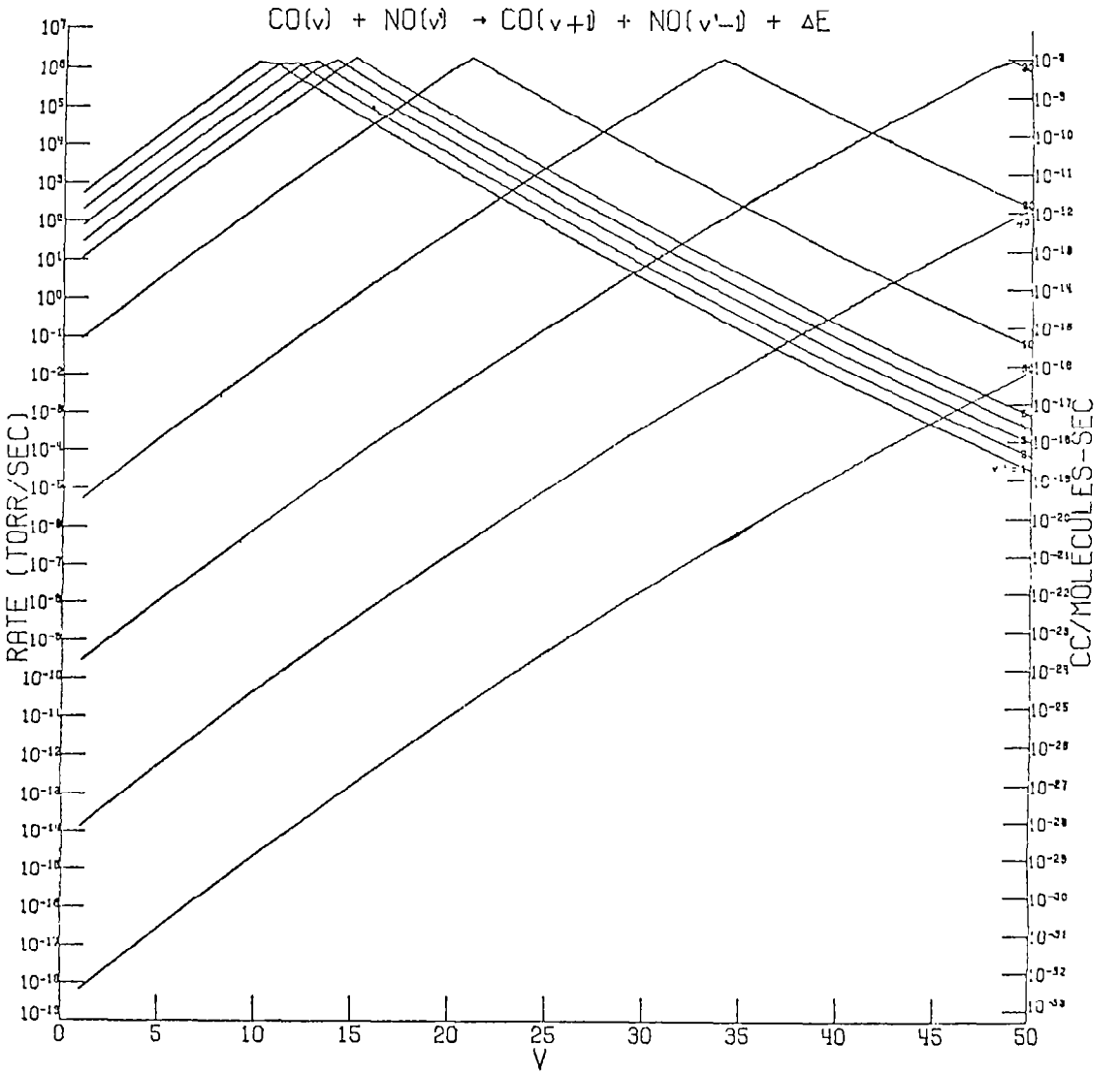

Fig. 1 Vibrational Transfer Rates in NO-CO Mixture.

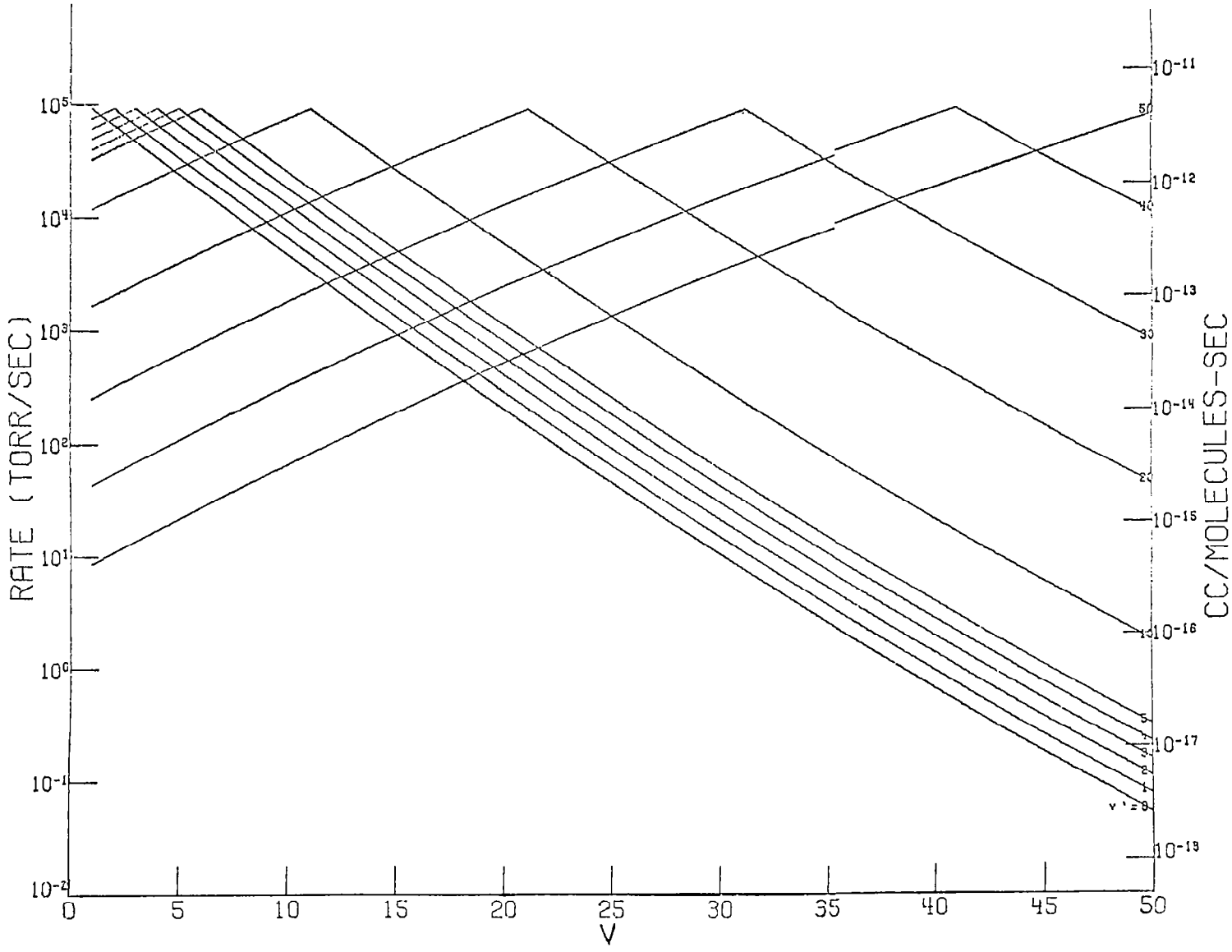

Fig. 2 Vibrational Transfer rates in CO-CO Mixture.

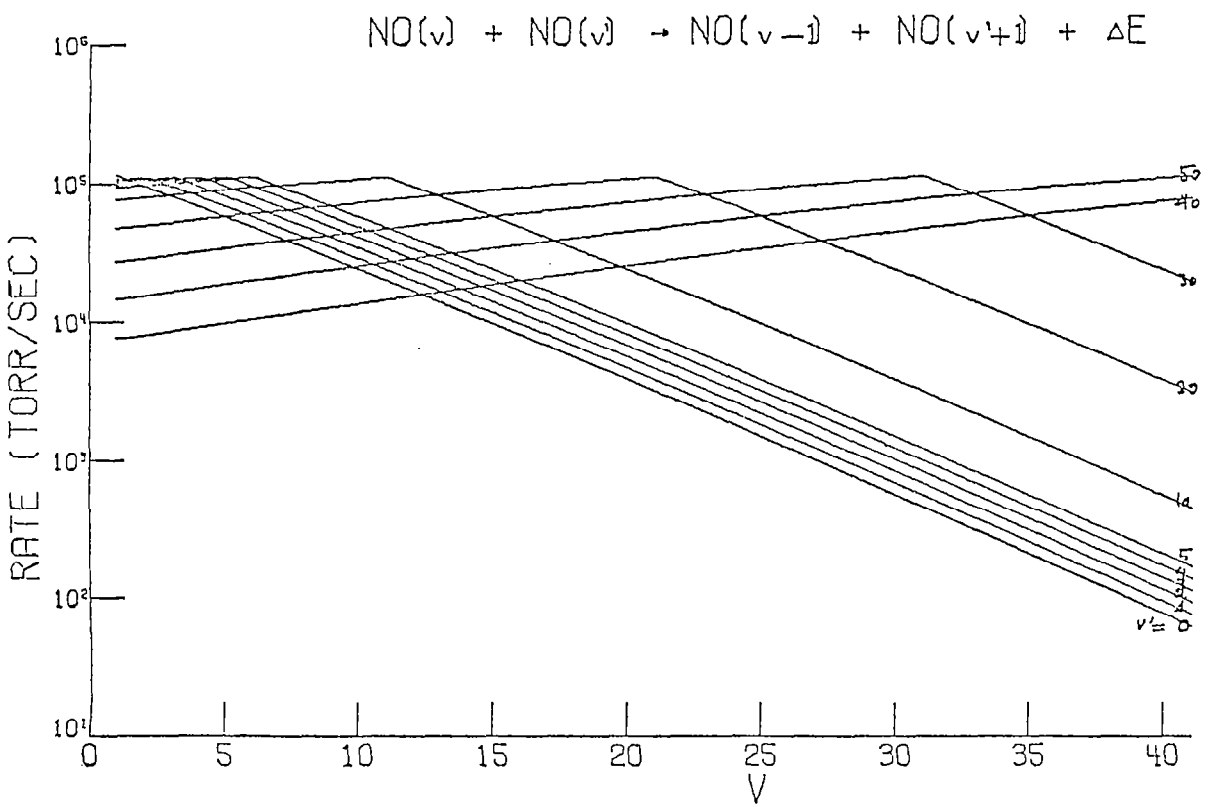

Fig. 3 Vibrational Transfer Rates in NO-NO Mixture.